

**THE STUDY OF AGAR BINDER AND SUPER P ADDITIVE IN  
POROUS ZINC ANODE FOR ZINC-AIR BATTERIES**

**by**

**MOHAMAD NAJMI MASRI**

**Thesis submitted in fulfilment of the requirements**

**for the degree of**

**Doctor of Philosophy**

**MAY 2013**

## ACKNOWLEDGEMENTS

In the name of Allah, the Most Beneficent and the Most Merciful, all praise to Allah for the strengths and His blessing in completing this Doctor of Philosophy program successfully.

I would like to extend my warmest appreciation to my supervisor, Assoc. Prof. Dr. Ahmad Azmin Mohamad, for his valuable contributions, incredible advice, patience and understanding during the research and writing of this thesis. His wisdom, knowledge and commitment to the highest standards have inspired and motivated me. His assistance and support during the process of learning has been conducted in an extremely professional and amicable manner, of which I am grateful. Not forgotten, my appreciation to my co-supervisor, Prof. Dr. Azizan Aziz for his support and guidance. The guidance is well-appreciated and I deeply believe that one could not possibly reach this far without such respectable supervision.

I would like to express my gratitude to the School of Materials and Mineral Resources Engineering, Universiti Sains Malaysia for accommodating me during the conduct of my studies and for allowing me to use related facilities and equipment; the technical staff, Suhaimi Sulong, Meor Mohamad Noh Abdul Majid, Mohamad Zaini Saari and Mohd Halim Hassan and Muhammad Khairi Khalid; and the administration staff, Noor Hakishah Samsudin and Jamilah Taib who have also assisted me tremendously.

My real appreciation and thanks to my lab mates; Muhammad Firdaus Mohd Nazeri, Aliyah Jamaludin, Jeremy Koh, Tan Wee Ching, Siti Salwa Alias, Muhammad Ghaddafy Affendy, Lee Liu Mei and Haswani Alias, who have been giving me pieces of advice and encouragement unconditionally. Last but not least to my friends who are always willing to help when I encountered difficulties. Thanks for believing in me when I did not believe in myself.

I would also to thank the Ministry of Science, Technology, and Innovation, Malaysia for sponsoring the National Science Fellowship, and Universiti Sains Malaysia for providing the Research University Postgraduate Research Grant Scheme, which supported me financially during this study.

My deepest gratitude goes to my beloved parents, for their encouragement and prayers. Finally, my sincere gratitude is offered to my wife, Nurrol Naduwa for her constant supports, compromise and understanding during my PhD study.

*MOHAMAD NAJMI MASRI*

*May 2013*

## TABLE OF CONTENTS

ACKNOWLEDGEMENTS.....	ii
TABLE OF CONTENTS.....	iv
LIST OF TABLE.....	viii
LIST OF FIGURE.....	ix
LIST OF ABBREVIATIONS.....	xiv
LIST OF SYMBOLS.....	xvi
ABSTRAK.....	xviii
ABSTRACT.....	xix
CHAPTER 1 - INTRODUCTION.....	1
1.1 Background.....	1
1.2 Problem statement.....	3
1.3 Objectives.....	5
1.4 Scope of Work.....	5
1.5 Organization of Thesis.....	6
CHAPTER 2 - LITERATURE REVIEW.....	7
2.1 Introduction.....	7
2.2 Zinc-air Batteries.....	7
2.2.1 Components of Zinc-air Battery.....	9
2.2.2 Chemistry of Zinc-air Batteries.....	13
2.2.3 Classification of Anode in a Zinc-air Battery.....	16
2.3 Design of the Battery.....	17
2.4 Porosity and Surface Area.....	20
2.5 Classification of Porous Zinc Anode.....	22
2.5.1 Zinc Electrodeposition.....	23
2.5.2 Zinc Fibers.....	26

2.5.3	Zinc Lamination .....	28
2.5.4	Zinc Powder .....	29
2.6	Porous Zinc Binder .....	35
2.6.1	Types of Binder .....	37
2.6.2	Behaviour of the Binder .....	38
2.6.3	Binder Materials .....	41
2.6.4	Agar binder .....	42
2.7	Porous Zinc Additives .....	44
2.7.1	Properties of the Additive .....	46
2.7.2	Additive Materials .....	47
2.7.3	Super P Additive .....	49
2.8	Characteristics of the Binder .....	52
2.9	Porous Zinc Anode Characterizations .....	56
2.10	Characteristic of Zinc-air Battery's Performance .....	59
2.10.1	Discharge and Capacity .....	59
2.10.2	Current-Voltage and Power Density-Current Density .....	63
2.10.3	Open Circuit Voltage .....	66
CHAPTER 3 - METHODOLOGY .....		69
3.1	Introduction .....	69
3.2	Materials and Experimental Apparatus .....	69
3.3	Preparation of Agar Binder .....	71
3.4	Characterization of Agar Binder .....	72
3.4.1	Bulk Resistance and Conductivity of Agar Binder .....	72
3.4.2	Linear Sweep Voltammetry .....	75
3.5	Preparation of Porous Zinc Anode .....	75
3.5.1	Porous Zinc Anode: Effect of Potassium Hydroxide-Agar Binder .....	75
3.5.2	Porous Zinc Anode: Effect of Super P additive .....	77
3.6	Characterization of Porous Zinc Anode .....	78
3.7	Preparation of Sago-6 M Potassium Hydroxide Gel Electrolyte .....	81
3.8	Preparation of Air-cathode .....	82
3.9	Preparation of Zinc-air Battery Employing Porous Zinc Anode .....	82
3.10	Characterizations of Zinc-air Battery .....	84
3.10.1	Discharge Characterization .....	84

3.10.2	Current–Voltage and Current density–Power density Characterization .....	85
3.10.3	Open Circuit Voltage Characterization.....	85
3.11	Flow Chart of the Experimental.....	86
CHAPTER 4 - RESULTS AND DISCUSSION .....		87
4.1	Background .....	87
4.2	Effect of Adding Potassium Hydroxide to Agar binder.....	88
4.2.1	Binder Properties: Agar + Potassium Hydroxide.....	88
4.2.1.1	Bulk Resistance Properties.....	88
4.2.1.2	Conductivity Properties .....	95
4.2.1.3	Window stability properties for Zn-air Application .....	99
4.2.2	Porous Zinc Anode employing Agar-Potassium Hydroxide Binder Properties .....	100
4.2.2.1	Morphological Properties.....	101
4.2.2.2	Structural Properties.....	108
4.2.3	Electrochemical Analysis.....	110
4.2.3.1	Discharge Analysis .....	111
4.2.3.2	Power Density-Current Density Analysis.....	114
4.2.3.3	Open Circuit Potential Analysis.....	117
4.3	Effect of Super P Addition to Porous Zinc Anode .....	118
4.3.1	Electrochemical Analysis.....	118
4.3.1.1	Discharge Analysis .....	119
4.3.1.2	Power Density-Current Density Analysis.....	122
4.3.1.3	Open Circuit Potential Analysis.....	125
4.3.2	Porous Zinc Anode employing Super P Additive Properties.....	126
4.3.2.1	Morphological Properties.....	126
4.3.2.2	Structural Properties.....	136
CHAPTER 5 - CONCLUSION AND RECOMMENDATION .....		140
5.1	Conclusion .....	140
5.2	Recommendation .....	141
REFERENCES .....		144

APPENDIX A .....	166
APPENDIX B.....	167
APPENDIX C.....	168
APPENDIX D .....	169
APPENDIX E.....	170
APPENDIX F .....	171
APPENDIX G .....	175
APPENDIX H .....	176
APPENDIX I.....	178
LIST OF PUBLICATION.....	180

## LIST OF TABLE

		Pages
Table 2.1	The summary of porous Zn anodes	25
Table 2.2	Some parameters obtained from the discharge characterization for Zn-air batteries	63
Table 3.1	Material composition of agar binder	71
Table 3.2	Composition of anode materials	77
Table 4.1	Average of bulk resistance and intersection angle of agar binder with different KOH concentrations	90



## LIST OF FIGURE

		Pages
Figure 2.1	Schematic diagram of the basic configurations of a Zn-air battery (Lee et al., 2011)	10
Figure 2.2	Layers of air-cathode with different states of current collector; (a) internal and (b) side	11
Figure 2.3	The illustration on behaviour of oxygen from atmosphere into the air-cathode in Zn-air battery (Eom et al., 2006)	12
Figure 2.4	A collection of ZnO SEM images (Wang, 2004)	16
Figure 2.5	The Classification of anode utilization in Zn-air battery	16
Figure 2.6	Schematic diagram of cross-section commercial Zn-air battery (Energizer, 2013)	19
Figure 2.7	Condition of porous Zn anode, (a) before and after discharge as function of range in between the anode and air-cathode; (b) ideal and (c) inferior range	20
Figure 2.8	The basic design of (a) plate/foil, and porous Zn anode; (b) deposition, (c) fiber, (d) laminated/compressed and (e) powder	23
Figure 2.9	SEM images of the final products of Zn deposit morphologies (Wang et al., 2006b)	25
Figure 2.10	SEM image of typical sample Zn fibers (Zhang 2006)	26
Figure 2.11	The procedure to manufacture a porous Zn anode (Zhang, 2004)	27
Figure 2.12	Zinc lamination type; (a) ancient and (b) advanced (Erisman and Brown, 1981)	29
Figure 2.13	Porosity condition in porous Zn anode; (a) isolated particle, (b) lose contact particle and (c) optimum particle arrangement	30
Figure 2.14	SEM micrograph of Zn powder (Cho and Fey, 2008)	32
Figure 2.15	The qualitative relationship between conductivity and porosity (Zhang, 2006)	33

Figure 2.16	Relationship between porosity and effective surface area for porous Zn anode (Zhang, 2006)	35
Figure 2.17	Illustrations of different binder mechanisms on active particles: (a) direct binding and (b) indirect binding	37
Figure 2.18	Visualizations of binder behaviour: (a) ideal and (b) unacceptable binder	39
Figure 2.19	The chemical structure of agar (Mishra et al., 2011a)	43
Figure 2.20	Schematic illustration of behaviour of conventional anode; (a) before and (b) post discharge, with additive in Zn porous anode system; (c) before and (d) post discharge	45
Figure 2.21	SEM images of porous Zn anode with graphite powder (Othman et al, 2002b)	49
Figure 2.22	TEM images of Super P powder (Gnanamuthu and Lee, 2011a)	51
Figure 2.23	Electrical conductivity of various materials (Carraher, 2010)	53
Figure 2.24	Effect of the KOH concentration on conductivity of GPE and KOH aqueous solution (Iwakura et al., 2002)	54
Figure 2.25	LSV curves of chitosan-NH <sub>4</sub> NO <sub>3</sub> -EC at various temperatures (Ng and Mohamad, 2008)	56
Figure 2.26	SEM micrograph of Zn after discharge (Yang et al., 2004)	58
Figure 2.27	XRD pattern after discharge of Zn-air battery consisting porous Zn anode (Othman et al., 2002b)	58
Figure 2.28	Discharge profiles of Zn-air battery as function of time or specific discharge capacity	60
Figure 2.29	Zn-air batteries discharge profiles using air-cathode based on AgNP-SWNTs with AgNPs of different sizes at constant resistance of 1 k $\Omega$ (Wang et al., 2010)	61
Figure 2.30	Basic plot of $I-V$ and $J-P$	64
Figure 2.31	$I-V$ and $J-P$ curves of Zn-air battery employing 2.8 and 6 M electrolyte concentrations (Othman et al., 2002b)	65

Figure 2.32	$V_{oc}$ for Zn-air battery; (a) typical curve and (b) $V_{oc}$ value takes as in the discharge curve	66
Figure 2.33	$V_{oc}$ of Zn-air battery for 24 h (Mohamad, 2006)	68
Figure 3.1	Flow-chart of agar binder preparation	72
Figure 3.2	Nylon casing used for conductivity measurement; (a) separate components and (b) assembled casing	74
Figure 3.3	Schematic diagram of the porous Zn anode prepared	76
Figure 3.4	Flow chart of the porous Zn anode preparation	76
Figure 3.5	Flow chart of the porous Zn anode preparation with added Super P	78
Figure 3.6	Cross-sectional Illustration of the preparation of porous Zn anode sample	80
Figure 3.7	Flow-chart of sago-6 M KOH gel electrolyte preparation	81
Figure 3.8	Illustration of the Zn-air battery casing; (a) separate and (b) assembling of components	83
Figure 3.9	Flow chart of methodology	86
Figure 4.1	Nyquist plot of pure agar	91
Figure 4.2	Nyquist plots of agar with various KOH concentrations	92
Figure 4.3	Logarithmic imaginary impedance as a function of frequency with the increase of KOH	94
Figure 4.4	Conductivity of agar as a function of the KOH concentration	96
Figure 4.5	Schematic diagram of OH <sup>-</sup> in agar binder	97
Figure 4.6	Linear sweep voltammetry curves of agar binder with various concentration of KOH	100
Figure 4.7	Image of agar (a) granular and (b) gel	101
Figure 4.8	FESEM Image of granular agar	101

Figure 4.9	FESEM micrograph of Zn powder	102
Figure 4.10	FESEM micrograph of cross-section of porous Zn anode (a) inner surface [500 X] and (b) a close-up appearance	104
Figure 4.11	FESEM micrographs of (a) Zn-pure agar, and Zn with various KOH concentration of (b) 0.2 M, (c) 0.4 M and (d) 0.6 M	106
Figure 4.12	FESEM cross-section micrographs of Zn particles with (a) pure agar [3kX], (b) 0.2 M [5 kX], (c) 0.4 M [3kX] and (d) 0.6 M KOH	107
Figure 4.13	Illustration of the oxide thickness as a function of KOH concentration	108
Figure 4.14	Comparison of the XRD peaks of (a) pure agar, (b) Zn powder, and Zn with (c) pure agar, (d) 0.2 M, (e) 0.4 M and (f) 0.6 M KOH	109
Figure 4.15	Typical discharge profile of Zn-air batteries at 100 mA with different concentrations of KOH in the agar binder	111
Figure 4.16	Plot of the I-V curves for the Zn-air batteries as a function of KOH concentration in agar binder	115
Figure 4.17	Plot of the J-P curves for the Zn-air batteries at different KOH concentration in agar binder	116
Figure 4.18	Open circuit potential of Zn-air batteries with various KOH in the agar binder	118
Figure 4.19	Discharge profiles of Zn-air batteries at constant current of 100 mA as function of Super P concentration: (a) Zn pure, (b) Zn1C, (c) Zn2C, (d) Zn3C and (e) Zn4C	120
Figure 4.20	Conversion efficiency of Zn porous anode as function of Super P in Zn-air batteries system compared to the theoretical specific discharge capacity	121
Figure 4.21	Plot of the <i>I-V</i> curves for the Zn-air batteries at different concentrations of Super P	123
Figure 4.22	Plot of the <i>J-P</i> curves for the Zn-air batteries at different Super P concentrations	124
Figure 4.23	Open circuit potential of Zn-air batteries with various compositions of Super P in the porous Zn anode: (a) Zn pure,	126

	(b) Zn1C, (c) Zn2C, (d) Zn3C and (e) Zn4C	
Figure 4.24	The FESEM micrographs of (a) dried agar binder film [5 kX], (b) Zn powder [5 kX] and (c) Zn p	127
Figure 4.25	FESEM micrographs of Super P	129
Figure 4.26	The FESEM micrographs of porous anode prior to discharge: (a) Zn1C, (b) Zn2C, (c) Zn3C and (d) Zn4C [30kX]. Initial area of samples are highlighted in images (inset [5kX])	130
Figure 4.27	The FESEM micrographs of porous Zn anode after discharge: (a) Zn pure, (b) Zn1C, (c) Zn2C, (d) Zn3C and (e) Zn4C	132
Figure 4.28	TEM morphology of (a) Super P, before discharge anodes; (b) Zn pure and (c) Zn2C, after discharge anodes (d) Zn pure and (e) Zn2C	134
Figure 4.29	The arrangement in the porous Zn anode (a) actual TEM image of Zn2C and, (b) a graphical illustration of microstructure in porous Zn anode made of Zn and Super P powder	135
Figure 4.30	The XRD pattern of Super P	136
Figure 4.31	The XRD patterns of porous Zn anode before discharge: (a) Zn pure, (b) Zn1C, (c) Zn2C, (d) Zn3C and (e) Zn4C	138
Figure 4.32	The XRD patterns of porous Zn anode post discharge: (a) Zn pure, (b) Zn1C, (c) Zn2C, (d) Zn3C, and (e) Zn4C	139

## LIST OF ABBREVIATIONS

AB	Acetylene black
AgNP	Silver nanoparticle
Al-air	Aluminium-air
Cu	Copper
FESEM	Field emission scanning electron microscope
FRA	Frequency response analyser
Fe-air	Iron-air
GPE	Polymer gel electrolyte
H <sub>2</sub> O	Water
ICDD	International Centre of Diffraction Data
KOH	Potassium hydroxide
Li-air	Lithium-air
Li-ion	Lithium-ion
LiCoO <sub>2</sub>	Lithium cobalt oxide
LiOH	Lithium hydroxide
LSV	Linear sweep voltammetry
MnO <sub>2</sub>	Manganese oxide
Mg-air	Magnesium-air
NaOH	Sodium hydroxide
Ni	Nickel
NMP	1-methyl-2-pyrrolidone
OH <sup>-</sup>	Hydroxide
O <sub>2</sub>	Oxygen
PTFE	Polytetrafluoroethylene
PC	Polycarbonate

PVDF	Polyvinylidene fluoride
SEM	Scanning Electron Microscopy
SDBS	Sodium dodecyl benzene sulfonate
SiC	Silicon carbide
SWNT	Single-walled carbon nanotube
TEM	Transmission Electron Microscopy
$V_{oc}$	Open circuit voltage
XRD	X-ray Diffraction Spectroscopy
Zn	Zinc
Zn-air	Zinc-air
ZnO	Zinc oxide
$Zn(OH)_4^{2-}$	Zincate

## LIST OF SYMBOLS

%	Percentage
~	Approximately
$\theta$	Theta
$\sigma$	Ionic conductivity
<	Less than
>	More than
$\leq$	Less than or equal to
$\lambda^\circ$	Ionic molar conductivity
°	Degree
A	Ampere
$A\ m^{-2}$	Ampere per square meter
°C	Degree Celsius
ca.	Approximately
cm	Centimetre
d	Day
e.g.	For example
$f$	Frequency
g	Gram
h	Hour
i.e.	That is
$I$	Current
$J$	Current density
kg	Kilogram
L	Litre
M	Molar



m	Meter
min	Minute
mL	Millilitre
mm	Millimetre
nm	Nanometer
$P$	Power density
$R_b$	Bulk resistance
s	Second
t	Thickness
$V$	Voltage
wt%	Weight percent

# **KAJIAN MENGENAI PENGIKAT AGAR DAN BAHAN TAMBAH SUPER P DALAM ANOD ZINK BERLIANG UNTUK BATERI ZINK-UDARA**

## **ABSTRAK**

Bateri zink-udara (Zn-udara) telah difabrikasi menggunakan anod Zn berliang, katod-udara dan elektrolit gel 6 M KOH-sagu. Anod Zn berliang telah disediakan dengan campuran serbuk Zn dan pengikat agar-KOH pada kepekatan yang berbeza untuk mencapai kekonduksian dan ciri-ciri fizikal yang dikehendaki. Agar adalah polimer semulajadi, mudah didapati, mudah disediakan, murah, tidak mencemarkan alam sekitar dan boleh membentuk gel. Kehadiran KOH menyebabkan pertumbuhan struktur jarum ZnO yang meliputi bahan Zn-aktif. Keputusan menunjukkan bahawa pengikat Zn-agar tanpa KOH memberikan keupayaan nyahcas tertinggi iaitu 505 mAh·g<sup>-1</sup>. Walau bagaimanapun, kapasiti nyahcas menurun dengan peningkatan KOH. Selain itu, prestasi elektrokimia bagi bateri meningkat dengan kehadiran Super P. Antara kelebihan Super P adalah keaslian yang tinggi, luas permukaan tinggi dan struktur yang sempurna. Kehadiran bahan tambah Super P dalam anod Zn berliang meningkatkan prestasi nyahcas dan kestabilan pada voltan bateri Zn-udara. Kapasiti nyahcas dan ketumpatan kuasa bagi anod Zn yang mempunyai 2 wt% Super P adalah 776 mAh·g<sup>-1</sup> dan 20 mW·cm<sup>-2</sup>, masing-masing. Imej morfologi dan sifat-sifat struktur juga dianalisis untuk menyokong pemerhatian ini. Super P menjadi penghubung antara serbuk Zn dan meningkatkan prestasi elektrokimia bateri Zn-udara.

# THE STUDY OF AGAR BINDER AND SUPER P ADDITIVE IN POROUS ZINC ANODE FOR ZINC-AIR BATTERIES

## ABSTRACT

A zinc-air (Zn-air) battery was fabricated using porous Zn anode, an air cathode, and 6 M KOH-sago gel electrolyte. The porous Zn anode was prepared by mixing Zn powder and agar binder at different concentrations to achieve the desired conductivity and physical properties. Agar is an abundant natural polymer that does not require tedious and costly processing or preparation. Agar is also a gel-forming environmental friendly material. Meanwhile, the presence of KOH causes the growth of ZnO needle structures to cover the Zn-active material. Zn-agar binder without KOH produced the highest discharge capacity of  $505 \text{ mAh}\cdot\text{g}^{-1}$ . By contrast, the addition of KOH reduced the discharge capacity. The introduction of Super P improved the electrochemical performance of the batteries. The advantages of using Super P in batteries include high purity, large area, and highly structured body. The use of Super P additive in porous Zn anode enhanced the Zn-air battery discharge capacity because of the efficient and better voltage stability obtained from such an anode. The specific discharge capacity and power density of Zn anode with 2 wt% Super P were  $776 \text{ mAh}\cdot\text{g}^{-1}$  and  $20 \text{ mW}\cdot\text{cm}^{-2}$ , respectively. Morphological images and structural properties were also analyzed to support these observations. Super P acted as a bridge in the Zn powders and improved the electrochemical performance of the Zn-air batteries.

# CHAPTER 1

## INTRODUCTION

### 1.1 Background

Concerns on fluctuating prices of oil and serious environmental issues emphasize the urgent need for alternative energy (Anisur et al., 2013; Bernardes et al., 2004; Espinosa et al., 2004; Sayilgan et al., 2009). Recently, the demand for portable electronic devices has been increasingly driven by energy and power density sources (Dillon and Sun, 2012). The field of electrochemical energy sources has undergone positive development in the last decade. Metal-air batteries have also received considerable attention (Kraytsberg and Ein-Eli, 2012). Among all metal-air battery systems, the Zn-air battery shows high potential as an alternative energy storage device.

Zn-air batteries possess a unique set of attributes, including abundance, low cost, low toxicity, flat discharge, long shelf life, ease in handling, and high theoretical specific energy density ( $1,084 \text{ Wh}\cdot\text{kg}^{-1}$ ) (Lee et al., 2011). Generally, Zn-air batteries are composed of three major parts, namely, Zn as anode, air-cathode, and alkaline electrolyte. The electrolyte used in a Zn-based battery is predominantly aqueous alkaline electrolyte, such as potassium hydroxide (KOH), sodium hydroxide (NaOH), and lithium hydroxide (LiOH) (Sapkota and Kim, 2009).

The use of KOH as electrolyte in Zn-air systems has recently attracted attention because of the high ability of limiting ionic molar conductivity ( $\lambda^\circ$ ) of  $K^+$  ( $73.50 \text{ S}\cdot\text{cm}^2\cdot\text{mol}^{-1}$ ) compared with that of  $Na^+$  ( $50.11 \text{ S}\cdot\text{cm}^2\cdot\text{mol}^{-1}$ ) (Passaniti et al., 2011; Sapkota and Kim, 2010). Meanwhile,  $\lambda^\circ$  of  $OH^-$  is  $199.1 \text{ S}\cdot\text{cm}^2\cdot\text{mol}^{-1}$ , and the anions are commonly the charge carriers in alkaline systems (Giffin et al., 2012).

The air-cathode is responsible for determining battery activation. The air-cathode as a battery component provides unlimited oxygen ( $O_2$ ) supply as an active material, which can be obtained directly from the environment (Passaniti et al., 2011). These advantages contribute to the relatively small size and flexible designs for Zn-air batteries.

Another component that can enhance the high performance of a battery is the Zn anode. Zn anodes have two types, namely, Zn plate and porous Zn (Ye and Xu, 2007). Zn plates have a lower surface area than porous Zn anodes; the Zn plate is effectively moistened, and the usage of Zn-active material is optimized. By contrast, the porous Zn anode has better contact with the electrolyte because of its higher surface area, thus producing a promising performance rate for Zn-air batteries (Shaigan et al., 2010a).

Typically, a porous Zn anode is prepared from a powder mixture that includes Zn (main component), conductive powder, and binder. Porous Zn anodes can be fabricated using various methods, such as roll-bonding or compression, electrodeposition, and paste drying. Among these processes, paste drying is the simplest technique with promising outcomes.

## 1.2 Problem statement

Recently, a considerable number of studies based on porous Zn anode for Zn-air batteries have emerged (Othman et al., 2002a; Othman et al., 2002b; Ye and Xu, 2007). The development of Zn-air battery systems has shown great improvement from year to year. However, systematic and detailed studies on the use of binders are yet to be found in the literature.

The binder has an important function in tethering; it prevents the absolute disintegration of the active materials, which are normally fine powders or particles (Pejovnik et al., 2008). The binder functions not only as a highly adhesive agent but also as an effective dispersion medium for the active material (Huang et al., 2008a). Polytetrafluoroethylene (PTFE) is the most used binder for Zn-air batteries. Polycarbonate (PC) and sodium silicate have been recently discovered as binders as well (Hilder et al., 2009; Hilder et al., 2012).

Agar binder is introduced to emphasize green material alternatives to polymeric binders such as PTFE and PC. Othman et al. (2002b) introduced agar as a binder that can be used for preparing porous Zn anodes. Moreover, the addition of a few drops of KOH has been reported to enhance the conductivity of the agar binder; however, the exact value of KOH concentration was not specified. No systematic study has explored the effect of KOH addition to the binder, as well as the consequent improvement of porous anodes for Zn-air batteries. A conductivity study on agar mixture with KOH was also considered to ensure quantitative conductivity measurement.

The passivation of Zn-active materials by the formation of zinc oxide (ZnO) during discharge, which limits the usage efficiency of Zn, is also a research interest. The use of additives for porous Zn anodes has been proposed in several studies to overcome this problem (Bass et al., 1988; Duffield et al., 1987a; Müller et al., 1998; Othman et al., 2002b). Hilder et al. (2012) showed that the network in Zn-air batteries is dependent on carbon content because carbon functions as a conductive link between isolated metal particles, thus activating the anode for electrochemical reaction.

In this study, agar-KOH paste was used as a binder for a porous Zn anode. The further improvement was focused on the effects of the addition of Super P to the porous Zn anode on the performance of Zn-air batteries. The porous Zn anode was prepared by mixing Super P and Zn powder in agar binder paste. The performance of the porous Zn anode was characterized by electrochemical investigations and supported by morphological and structural studies. This study aims to verify the effect of agar binder in conjunction with Super P addition to porous Zn anodes for enhancing the performance of Zn-air batteries.

### **1.3 Objectives**

The main objectives of this research are as follows:

- (i) To determine the optimum conductivity of agar and KOH binder,
- (ii) To study the electrochemical properties of porous Zn anode with agar-KOH in Zn-air batteries, and
- (iii) To determine the effect of Super P addition on the properties of porous Zn anodes in Zn-air batteries.

### **1.4 Scope of Work**

This research was performed in three stages. The initial stage involved the characterization of agar binder by conductivity and potential window. Then, agar binder in the porous Zn anode for a Zn-air battery system was studied. Subsequently, the effect of Super P addition was also determined by electrochemical characterization. Finally, morphological and structural analyses were also conducted.



## **1.5 Organization of Thesis**

This thesis is divided into several chapters. The literature review provides information and summarizes the results related to porous Zn anodes in Zn-air battery systems. The relationships between Zn-air batteries and other assessment criteria involved in porous Zn anodes, such as binder and filler, are also reviewed in Chapter 2. Chapter 3 describes the experimental procedures including sample preparation to characterization. The results and discussion are presented in Chapter 4. Finally, Chapter 5 concludes the study with several suggestions for further research.

## **CHAPTER 2**

### **LITERATURE REVIEW**

#### **2.1 Introduction**

This chapter presents the theories on which this research was based. The construction of Zn-air batteries using porous Zn anode, as well as the steps of its preparation, is also discussed. The relationships between Zn-air batteries and other assessment criteria involving porous Zn anodes, such as binder and filler, are also explained. Zn-air battery assessments with regard to porous Zn anodes are also included.

#### **2.2 Zinc-air Batteries**

Metal-air batteries are a unique battery technology. These batteries are also called "breathing batteries" because absorb oxygen from the environment. It is also similar to fuel cells because they represent a "marriage" between battery (the anode) and fuel cell (the cathode). In particular, metal-air batteries are different from other types of batteries because of the virtual limitless supply of air, which enables the batteries to offer many advantages compared with other batteries. In short, cathode active material is not stored in the battery. These batteries produce electrical energy through the electrochemical reaction between the oxygen ( $O_2$ ) present in air and the anode that is oxidized. The superiority of metal-air batteries over conventional types of batteries is based on the high specific energy.

Although Zn-air is one of the most popular metal-air batteries, other metal-air batteries have also been considered include:

- (i) *Lithium-air (Li-air)* – This battery has the highest energy storage density, but its use is limited by safety issues and fast degradation under ambient conditions. In particular, the highly reactive Li should be isolated from moisture (H<sub>2</sub>O) and O<sub>2</sub> that can permeate the anode. Thus, complex and stable long-term separator is required in this battery (Hummelshøj et al., 2010; Thapa et al., 2011; Yu. Aleshin et al., 2011; Zhang et al., 2010),
- (ii) *Aluminium-air (Al-air)* - This battery is low cost and innocuous. However, it generates a large amount of heat and is highly corrosive (hydrogen evolution reaction), which affects the efficiency of the anode (Li et al., 2007; Mohamad, 2008; Tang et al., 2004; Wang et al., 2010a),
- (iii) *Magnesium-air (Mg-air)* – Mg is abundant and lightweight. However, Mg undergoes rapid self-corrosion (Chen et al., 2006; Li et al., 2006; Ma et al., 2010; Sathyanarayana and Munichandraiah, 1981), and
- (iv) *Iron-air (Fe-air)* - Passivation during discharge and high self-discharge result in its thermodynamic instability in alkaline-based electrolyte (Hang et al., 2006; Hang et al., 2007; Ito et al., 2011; Watanabe et al., 2006).

Most Zn-air batteries are designed for low-rate applications, although a high-rate version is also available (Levy and Bro, 1994). Their uses range from electric bus application (Goldstein et al., 1999) to the smallest commercially available Zn-air battery, which is approximately 50 mm<sup>3</sup> in size (Heller, 2006). Zn-air batteries have been used for hearing aid applications since the mid-1980s (Neburchilov et al., 2010; Pytches, 1983; Read, 2002a; Root, 2010; Sparkes and Lacey, 1997; Zhang et al., 2008).

The unique properties of Zn-air batteries make them indispensable in military (Brownlee et al., 1969; Jamaludin et al., 2010; Knapp et al., 1969) and safety applications, such as railway signals (Culter, 1996; Pistoia, 2005; Pistoia, 2008). The emergence of sophisticated devices has stimulated new research work focusing on the longevity and energy density of batteries. Hence, longer durability, superior performance, dependability, and cost effectiveness are the properties of a good battery.

Electric Fuel Corporation promoted small-size versions of Zn-air primary batteries for use in mobile telephones. These batteries provide three to five times more "talk-time" than rechargeable batteries, which is useful when recharging is not readily possible. As a primary battery, the Zn-air battery can be used straight from the packet without the need for a preliminary charge (Goldstein et al., 1999). Latest developments on Zn-air batteries have also prompted the energy industries to produce commercial rechargeable Zn-air batteries (Badarulzaman et al., 2009; Masri, 2008; Pistoia, 2008; Zhang, 2004).

## 2.2.1 Components of Zinc-air Battery

Figure 2.1 shows the basic components of a Zn-air battery. A Zn-air battery consists of an alkaline electrolyte, and it operates using a steady supply of oxygen from air.  $O_2$  is reduced at the air-cathode, forming a hydroxyl ( $OH^-$ ) ion that migrates through the electrolyte to the Zn anode. This reaction produces electrons, which are transported through the external circuit to the air-cathode, thereby generating electricity. The  $OH^-$  ions react to form zinc oxide ( $ZnO$ ), which is a by-product of the reaction.

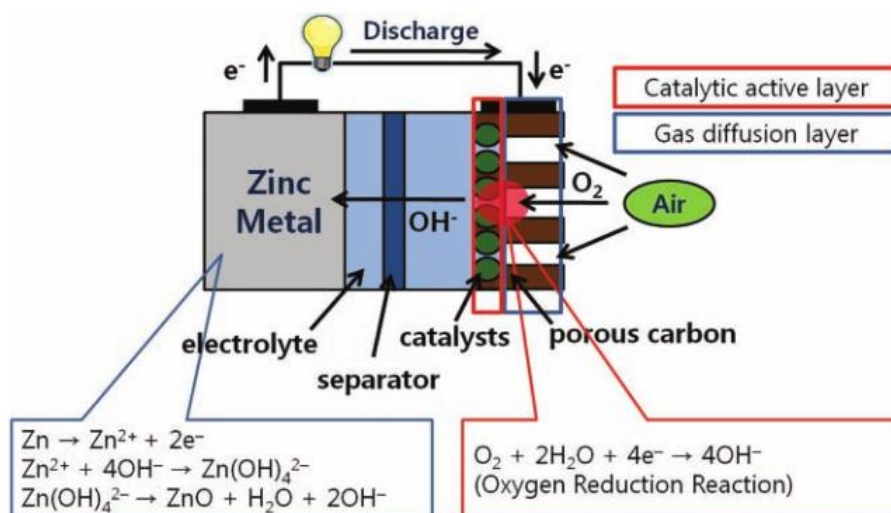


Figure 2.1: Schematic diagram of the basic configurations of a Zn-air battery (Lee et al., 2011)

The use of an air-cathode or gas diffusion electrode distinguishes Zn-air batteries from other batteries; battery weight is considerably reduced, resulting in a compact and simplified battery design (Barak, 1980; Chamran et al., 2007; Williford and Zhang, 2009; Zhang, 2004). Figure 2.2 demonstrates a schematic illustration of the basic components of different air-cathode designs. Air-cathodes reduce  $O_2$  to produce  $OH^-$ , which is soluble in an aqueous electrolyte.

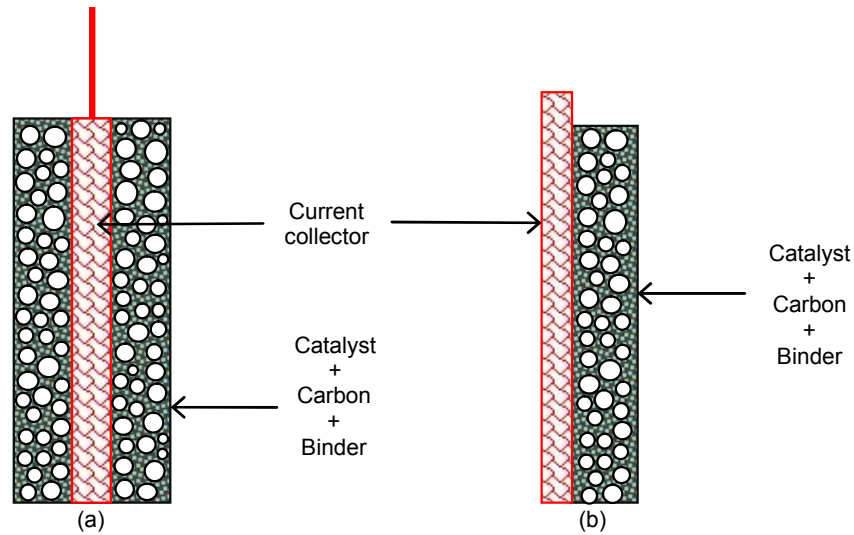


Figure 2.2: Layers of air-cathode with different states of current collector; (a) internal and (b) side

An air-cathode has huge hydrophobic channels to maximize  $O_2$  diffusion (Eom et al., 2006; Li et al., 2010). Chemical and dimensional stability, sufficient porosity, and high electronic conductivity are required in an air-cathode (Singhal and Gopalan, 2000). Typically, an air-cathode consists of four main materials, namely, the catalyst, carbon, current collector, and binder (Durkot et al., 2007; Wang and Zhou, 2010). The most widely reported catalyst is manganese oxide ( $MnO_2$ ) impregnated with carbon (Cao et al., 2003; Feng et al., 2005; Wei et al., 2000).

The infinite supply of  $O_2$  from the environment provides advantages to the Zn-air battery system. Figure 2.3 illustrates the air flow through the air-cathode material as it catalytically promotes the reduction of  $O_2$  in the electrolyte. Further concerns on  $O_2$  flowing into the air-cathode was studied by Eom et al. (2006). The air-cathode is generally durable and remains constant during Zn-air battery discharge (Mohamad, 2006a).

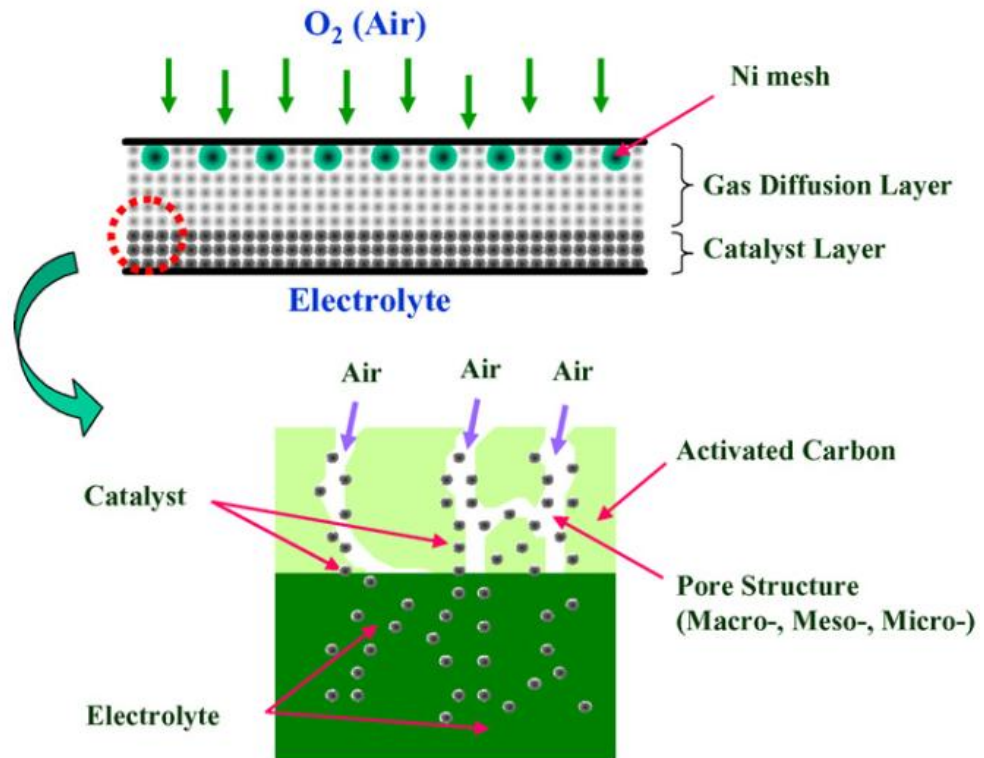


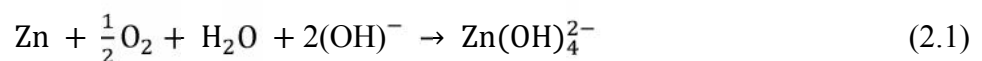
Figure 2.3: The illustration on behaviour of oxygen from atmosphere into the air-cathode in Zn-air battery (Eom et al., 2006)

The choice of electrolyte highly depends on the electrodes used. The characteristics of the electrolyte that must be considered are conductivity and viscosity (Blomgren, 1999). The majority of Zn-air batteries use aqueous alkaline solutions, particularly potassium hydroxide (KOH), because of its high conductivity and excellent ability to control the reduction of  $O_2$  ions into  $OH^-$  anions (Almeida et al., 2009; Barak, 1980; Dell and Rand, 2001; Dirkse and Kroon, 1971; Koscher and Kordesch, 2004; Miura et al., 1988; Putt and Merry, 1992; Pytches, 1983; Zhang, 1996; Zheng et al., 2004).

The capacity of Zn-air batteries is attributed to the type of air-cathode material and the concentration of KOH in the electrolyte. However, the anode is another key factor in determining battery performance (Akuto et al., 2001; Hang et al., 2005; Linden, 2001; Winter and Brodd, 2004; Yang et al., 2004). A number of factors must be considered to optimize the anode materials, such as the material cost for the alkaline battery (Koretz et al., 1995; Muller et al., 1998; Roundy et al., 2004), abundance of resources, non-toxicity (Chao et al., 2008; Chen et al., 2011; Chen et al., 2010; Vatsalarani et al., 2009), low equilibrium potential, and high over-potential of the reaction of hydrogen with Zn (Chao et al., 2008; Chen et al., 2011; Chen et al., 2010; Smedley and Zhang, 2007; Zheng et al., 2004).

### 2.2.2 Chemistry of Zinc-air Batteries

The Zn anode chemistry as the Zn-air battery discharges in an alkaline electrolyte (Linden and Reddy, 2001a; Reddy, 2010b) is represented by Equation 2.1:

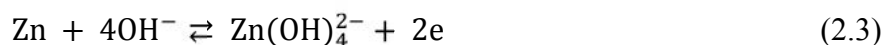


The reactions of Zn in Zn-air batteries during discharge are simultaneous, and the use of an oxygen-reducing catalyst in an air-cathode results in the reduction of the O<sub>2</sub> adsorbed from the surrounding air (Chang, 1963; Foller, 1986; Genies et al., 2003; Mohamad et al., 2003; Wang et al., 2010b; Wu et al., 2007; Yang and Zhou, 1995). The reactions are presented in Equation 2.2:





The reaction of the preliminary discharge at the Zn electrode can be expressed by Equation 2.3 (Reddy, 2010b):



This reaction proceeds until the zincate  $[\text{Zn}(\text{OH})_4^{2-}]$  ion reaches saturation point because the supersaturation rate is time dependent. This effect is caused by the solubility of the anion in the electrolyte. Thus, the stable solubility stage is exceeded upon complete discharge, which results in the formation of ZnO precipitate (Tan and Mohamad, 2010; Yap et al., 2009). This reaction can be presented as Equation 2.4:



The overall battery reaction may be simplified as Equation 2.5 (Chodosh et al., 1966; Chodosh et al., 1967; Cretzmeyer et al., 1976; Culter, 1996; Malone et al., 2004; Pistoia, 2008):



The tendency of Zn to corrode during battery storage remains a difficult problem that should be addressed. Hence, researchers have investigated the electrochemical reaction involved in alkaline solutions (Culter, 1996; Dirkse and Timmer, 1969; Zhang and Zhang, 2003). The predominant oxidized products of the

aforementioned reactions are generally believed to be  $\text{Zn(OH)}_4^{2-}$ . Nevertheless, most researchers believe that the passive films contain ZnO (Buchholz, 1980; Dirkse and Timmer, 1969; Goldstein and Koretz, 1998; Graedel, 1989; Rudd and Breslin, 2000; Yang et al., 2004).

The status of Zn can be identified by two different colors, namely, grey (fresh Zn) and white (incompletely discharged Zn). Deiss et al. (2002) claimed that ZnO could form and remain on the Zn electrode after discharge. Many researchers have proposed mechanisms of ZnO formation based on material, preparation, and methodology (Bockris et al., 1972; Cai and Park, 1996; Chang and Prentice, 1984; Chang and Prentice, 1989). The growth morphology enables the tuning of reaction conditions to obtain the desired properties, such as the shape and size (*ca.* nanoscale) of a material and even the by-product of the Zn-air battery system for a specific application.

The possible structures of ZnO include combs (Pan et al., 2005; Yang et al., 2002), rods (Boyle et al., 2002; Gonzalez-Valls and Lira-Cantu, 2010; Lee et al., 2007; O'Brien et al., 1996), spherulitic prisms (Verges et al., 1990), helices (Tian et al., 2002), porous structures (Wang et al., 2004), tetrapods (Al-Azri et al., 2010; Wang et al., 2004), belts (Kong et al., 2004; Kong and Wang, 2003), propellers (Gao and Wang, 2004), flowers (Al-Azri et al., 2010; Xu et al., 2009), wires (Al-Azri et al., 2010; Yang et al., 2002; Zhao et al., 2003), spheres (Alias et al., 2010; Verges et al., 1990), plates (Tian et al., 2002), rosettes (Tan and Mohamad, 2010), and needles (Mohamad, 2006; Othman et al., 2001b; Tan and Mohamad, 2010). Figure 2.4 shows the scanning electron microscopy (SEM) images of the examples of ZnO.

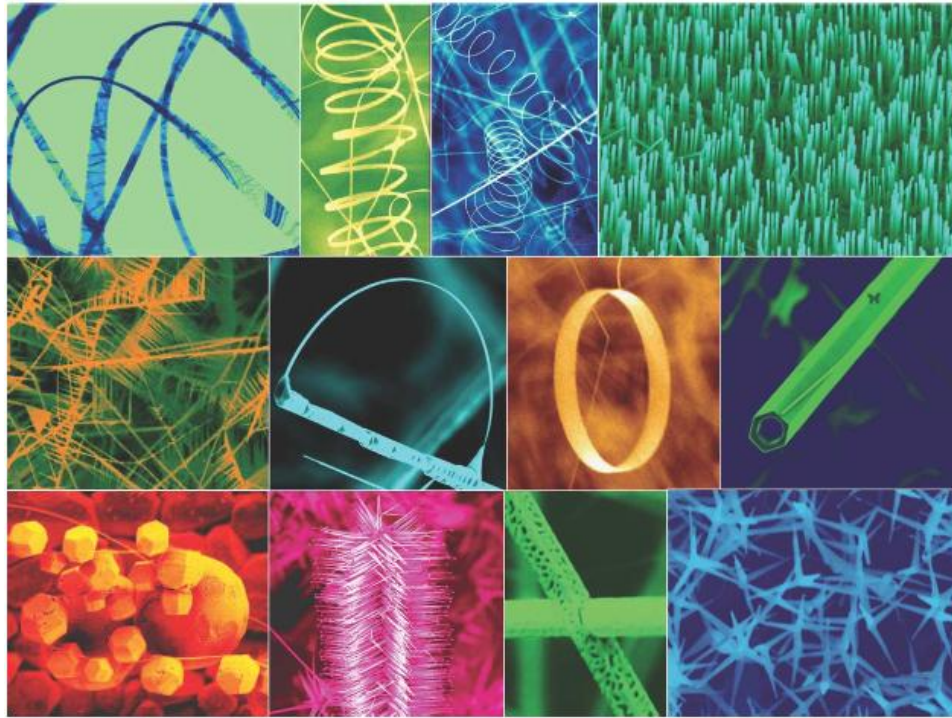


Figure 2.4: A collection of ZnO SEM images (Wang, 2004)

### 2.2.3 Classification of Anode in a Zinc-air Battery

Zn-air battery anodes are classified into two main groups, namely, solid and porous Zn. Zn powder, fiber, lamination, and deposition are included in the porous group. The classification of Zn-air anodes is summarized in Figure 2.5.

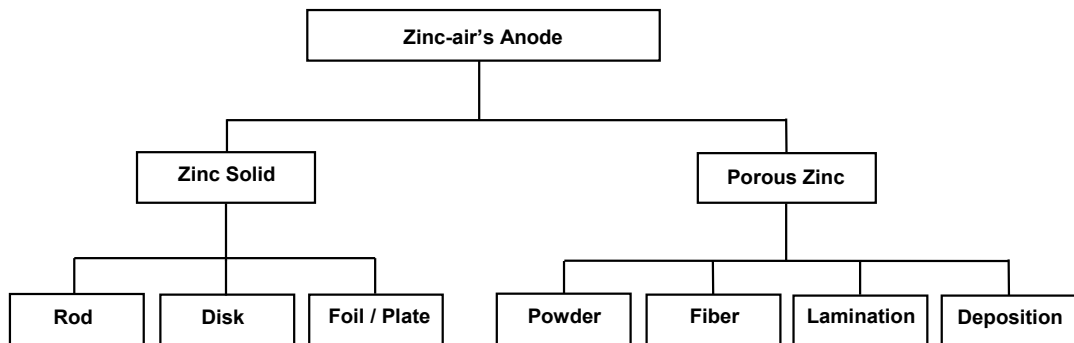


Figure 2.5: The Classification of anode utilization in Zn-air battery

Batteries with a porous anode normally demonstrate 40% higher capacity than those with planar Zn (Minakshi et al., 2010). The electrolytes flow more freely across the entire surface of Zn powder when the surface area is increased. However, a few stringent conditions involving the surface area of the materials used must be met in the fabrication of batteries. In particular, the surface area of Zn particles can affect the properties of the battery, such as (Stanley and Thornton, 2002):

- (i) Lifetime of the battery,
- (ii) Discharge rate of the battery, and
- (iii) Ease of preparation of the battery components.

A large surface area can result in very rapid anode degradation. Meanwhile, a very small surface area may not meet battery specifications. The discharge rate of a battery is also determined by the area of exposed surface (Sparkes and Lacey, 1997). Ease of preparation should also be considered, and this includes the adhesion performance of the paste (binder) used to produce neutral gaps between the active materials.

### **2.3 Design of the Battery**

The size, shape, performance, and design parameters of a battery are considered variables that can be customized for a variety of specific geometry and dependence functions. A battery can be placed at arbitrary locations within an electronic device. As a result, free design of electronic devices can be achieved in terms of available energy sources and may allow for new possibilities in performance, such as increased discharge capacity. Regardless of the shape and

design, the assembled battery should not suffer from electrolyte leakage or the premature entry of air. Hence, batteries are sealed in numerous ways to prevent leakage (Cheiky, 1995; R.M, 2000). Designs with bigger diameters and thinner walls are preferred. Other factors to be considered in designing batteries are air and electrolyte (Root, 2010).

The popular use of Zn-air batteries in battery research laboratories can be attributed to the stability of the battery materials. Cells for Zn-air batteries can be easily fabricated under ambient air and without the use of sophisticated equipment. The development in battery design focuses on three key objectives, namely:

- (i) Full Zn utilization for complete reaction,
- (ii) Maximization of the active area of the air-cathode to reduce  $O_2$ , and
- (iii) Determination of the functionality and cost of batteries.

Conventional Zn-air batteries have large volumes, usually around  $30 \text{ mm}^3$  (Chao et al., 2008). Hence, the recent trend in Zn-air battery design leans toward lighter, thinner, and smaller sizes. The two types of extensively developed commercial Zn-air batteries are the button cells and low-rate industrial batteries. The cross-section of button Zn-air batteries used for hearing aids is shown in Figure 2.6. Zn-air batteries offer a capacity advantage because of air-cathode mass, and their design is similar to that of Zn-mercuric oxide button cells. The battery design uses an anode paste of amalgamated Zn powder in a gelled KOH electrolyte (Knapp et al., 1969) and an air-cathode (Putt and Merry, 1992).

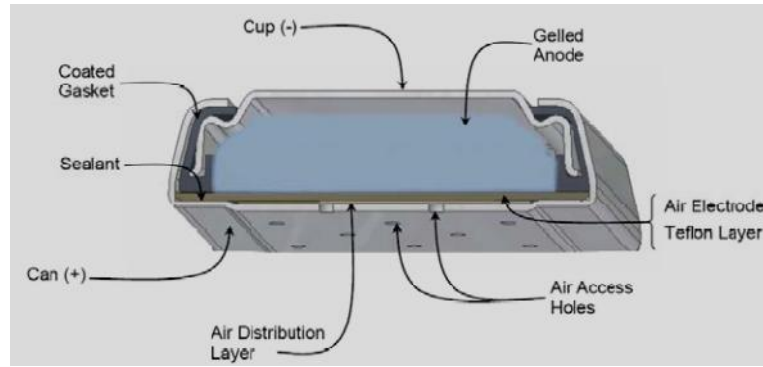


Figure 2.6: Schematic diagram of cross-section commercial Zn-air battery (Energizer, 2013)

Anode thickness is consistent with specific capacity requirements. Industrial Zn-air batteries are of a prismatic configuration and are also encased in molded plastic. This type of battery has a promising service life (2 years to 3 years), with a maximum continuous drain rate of  $\leq 1$  A (Putt and Merry, 1992). Another battery design suitable for military applications is reported elsewhere (Knapp et al., 1969).

Figure 2.7 demonstrates the condition that has always been a drawback to Zn-air battery design. The state of the porous Zn anode before discharge can be seen in Figure 2.7a. The growth of ZnO needles after discharge can cause an internal short circuit or leakage (Cooper and Krueger, 2006; Shaigan et al., 2010b); thus, the available space must be within an exact range to overcome this problem (Figure 2.7b). In small spaces, the continuous growth of ZnO needles connects the anode and the air-cathode (Figure 2.7c).

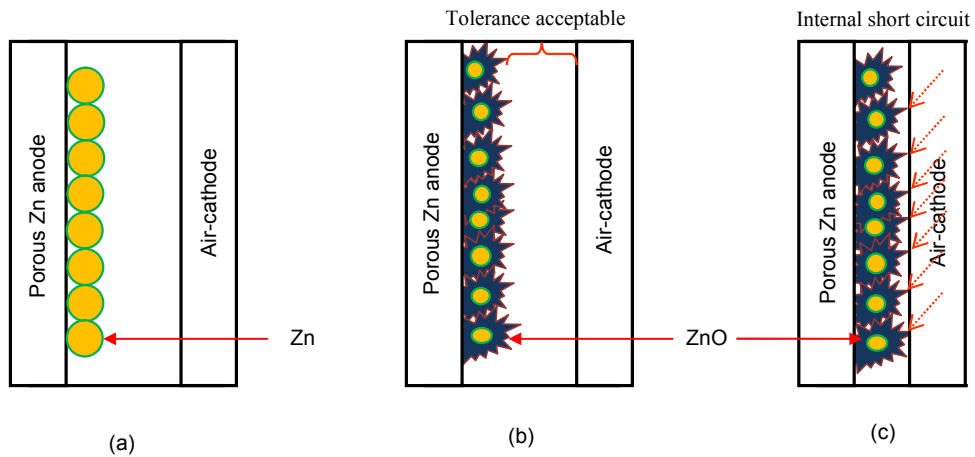


Figure 2.7: Condition of porous Zn anode, (a) before and after discharge as function of range in between the anode and air-cathode; (b) ideal and (c) inferior range

## 2.4 Porosity and Surface Area

A porous Zn anode system typically consists of an active material (Zn powder), additives, and binders. Additives increase the conductivity and life span of the active material. Binders essentially act as holders for the active material. Zn-air batteries typically use anodes made from powders of active materials, which is Zn, to obtain the highest possible surface area per unit weight or volume (Winter and Brodd, 2004). This method is highly useful in meeting the current demand for new and emerging miniature devices, which are being developed yearly, while increasing the surface area of the anode and the capacity of the battery.

The dispersion of porous Zn anode ingredients is controlled by several factors, such as the size and shape of the particle, density, volume fraction of individual components, and interparticle interaction (Hong et al., 2002). These elements affect the mixing efficiency of the paste preparation step, thus dispersing powder in the porous Zn anode. The specific surface area is defined as the area of the surface where the electrochemical reaction between the electrolyte and Zn occurs and produces an electric current (Hilder et al., 2009). The correlation can be simply expressed by Equation 2.6:

$$\text{Specific surface area} = \frac{\text{Effective surface area (m}^2\text{)}}{\text{Weight of active materials (g)}} \quad (2.6)$$

Another method used to calculate the surface area is based on micrograph image-processing software. The ImageJ software can also be used for simple processing. The calculation is based on the porous and solid images, and the observations are differentiated according to color. For this quantitative technique, evaluation depends only on the appearance of the micrograph rather than on that of the overall sample. The porosity can also be calculated according to the following Equation 2.7 (Othman et al., 2002b):

$$\text{Porosity} = \frac{V_{\text{pore}}}{V_{\text{total}}} \times 100\% \quad (2.7)$$



Porosity refers to the fractional volume that is not filled with solids. Porosity is determined by the binder concentrations described in Equation 2.7, where  $V_{\text{pore}}$  is the total pore volume within the electrode and  $V_{\text{total}}$  is the total electrode volume. Porosity and the distribution of porous space in the anode play a significant role in the anode performance in the batteries (Deiss et al., 2002), and their effects are mainly determined by the shape of the Zn particles and the design of the anode. Meanwhile, the important parameters that characterize the porous Zn anode are specific surface area, effective surface, porosity, and physical stability.

## 2.5 Classification of Porous Zinc Anode

The reported porosity percentage generally varies between 10% and 70% of the amount of anode (Knapp, 1968; Warszawski, 1979). However, the performance of porous Zn anodes depends on both the active materials and the processing parameters (Biegler et al., 1983; Maja et al., 2000; Wang et al., 2006a). Table 2.1 summarizes the classification of porous Zn anodes. Figure 2.8 also illustrates the common Zn anode designs. Figure 2.8a shows the Zn plate/foil (solid) commonly used in Zn-air research. Zn deposition (Figure 2.8b) can increase the active surface area similar to that in the fiber approach (Figure 2.8c). Laminated/compressed (Figures 2.8d) and powder porous (Figures 2.8e) Zn anodes are slightly similar, but their fabrication methods are different.

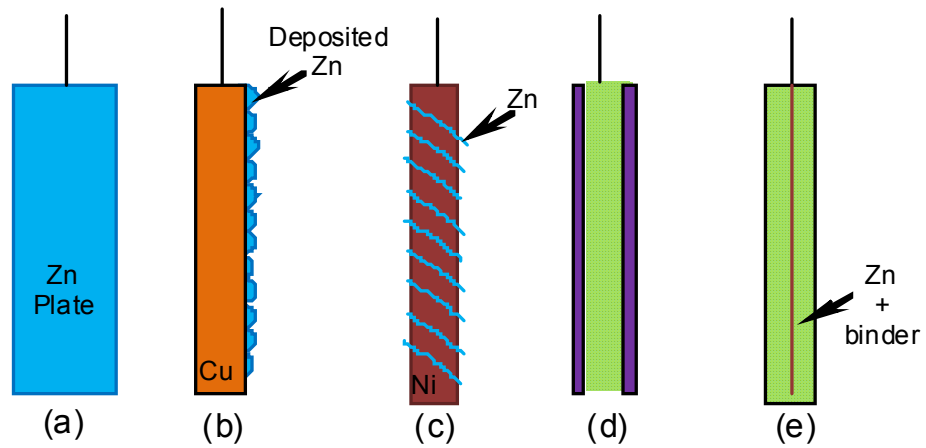


Figure 2.8: The basic design of (a) plate/foil, and porous Zn anode; (b) deposition, (c) fiber, (d) laminated/compressed and (e) powder

### 2.5.1 Zinc Electrodeposition

Electrodeposited Zn is considered as a type of porous Zn anode. Zn is known as one of the most electropositive metals (Koscher and Kordesch, 2004). Thus, pure Zn may be electrodeposited using an aqueous electrolyte, leading to the improvement in the surface area on the substrate (Freitas and De Pietre, 2005; Naybour, 1968; Pal and Chakravorty, 2006; Wang et al., 2006a). The Zn particles are deposited on the surface of the current collector, such as copper (Cu) or nickel (Ni).



Table 2.1: The summary of porous Zn anodes

Types	Processing	Zn Form	Ref.
Electrodeposition	Obtained by the current collector as deposited zincate.	Surface morphology; Spongy, dendrite, layer-like, mossy	Wang et al. (2006a)
Fiber	Anode porosity and shape according to the processes, including: i. Packaging ii. Pressing iii. Fusing iv. Molten rolling v. Cutting	Needle, wire, filament, strands, or threads	Headrick et al. (2002); Heller (2006); Zhang (2006)
Lamination	Continuous mesh or perforated. Anode porosity and shape dominance via rolling or stacking.	Sandwich, stack	Zhang and Zhang (2004); Zhang et al. (2001); Zheng et al. (2004)
Powder	Anode porosity as determined via gelling/binder and anode's shape controlled by the anode cavity/casing	Powder	Othman et al. (2002b)